# THE INFLUENCE OF SOME PARAMETERS IN ATMOSPHERIC PLASMA SPRAY OF POWDER 85Ni15Al ON THE PARTICLE VELOCITY

**Vu Duong**[1,*], **Le Hong Ky**[2]

DOI: http://doi.org/10.57001/huih5804.2024.168

## ABSTRACT

The work focuses on the effect of plasma spraying factors such as plasma current, plasma voltage, and air flow rate on particle velocity because the effectiveness of the coating is heavily dependent on it. The inclusion of ordinary air as the plasma-generating gas and the explanation of the mathematical model justifying the alteration of particle velocity are the innovative aspects of this work. The newly discovered regression function helps the mathematical model optimize the procedure to achieve the greatest particle velocity. The parameter validity study confirmed the good comparative adaptation between the mathematical model and the experiment results. The introduction paragraph explained why this study is necessary. The paragraph "Methodology" introduced the equipment, instrument for analysis, the chemical composition of the material 85Ni15Al. The paragraph "Experiment" focused on a series of experiments. The multi-criteria planning design helps to conclude the significance of all parameter and well adopted to the experiment.

***Keywords:*** *Particle velocity; atmospheric plasma spray; ordinary air; plasma generation gas; mathematical model; regression equation.*

---

[1] School of Engineering Technology, Duy Tan University, Vietnam
[2] Vinh Long University of Technology Education, Vietnam
[*] Email: duongvuaustralia@gmail.com

Received: 20/8/2023
Revised: 05/10/2023
Accepted: 25/5/2024

## 1. INTRODUCTION

The efficiency and productivity of atmospheric plasma spray (APS) are highly dependent on the mean temperature and velocity of the powder particle prior to impact with the substrate. Because the condition of the in-flight particle is very important, B. Guduri et al. offered their inquiry in depth to set up a stable and adaptable instrument for obtaining a consistent value [1]. In the experiment, the authors employed argon and hydrogen in a mixture with flow rates of 30 -60 standard liters per minute (slm) and 0 - 15slm, currents of 300 - 600A, voltages of 30 - 70V, and a plasma torch diameter of 8mm. The powder for spraying had a particle size of 30 - 100µm, but no mechanical composition or size distribution was given, despite the fact that particle size is important in this complicated operation. ANOVA analysis revealed that the current and flow rate of argon had a significant influence on particle velocity. Although the response functions have been adequately implemented, more study is required to create a robust controller.

The velocity of the particle takes precedence over temperature in the cold spray procedure. However, the spray distance and powder feed rate have a significant impact on particle velocity [2, 3]. The researchers identified the threshold velocity of the particle, beyond which it may bond to the substrate surface and form the coating. In any case, they do not present a quantitative relationship between particle velocity and some key technical characteristics. Because the critical velocity of the particle in spraying is thought to be a crucial element in bonding, the researchers in [4] studied particle behavior in the kinetic spraying of AlSi feedstock using the method Kurochkin et al. [5] developed to identify the critical velocity approaching 400m/s. It's worth noting that the particle with a maximum velocity greater than the crucial one will not be stuck to the substrate since the adhesion energy is less than the rebound energy. [6] performed a large number of supersonic plasma sprayings of ceramic powder (YZS) over the nickel-based superalloy GH 3030. They obtained a collection of data that included current, voltage, argon, hydrogen, feedstock feeding rate, spray distance, and velocity, but not the assessment and analysis of the parameters due to a lack of a regression relationship between them. From this vantage point, the optimum range of spraying settings to achieve maximum particle velocity and temperature is insufficient to persuade. In [7], an attempt was made to derive a new mathematical model that included particle and gas velocity, particle mass, gas density, particle diameter, and drag coefficient. They compared the experimental measurement using a dual-slit velocimeter to the 2-D axi-symmetric calculation of the flow through the nozzle and the 1D isentropic gas-dynamic equations computed for the identical nozzle shape. The particle size distribution caused a difference in the theoretical computation of particle velocity. The major discovery in their investigation is that particles with velocities greater than the critical velocity deposit, but bigger particles with lower velocities do not. The primary disadvantage of [8] is that the model based on Newton's second law does not address the technological parameters in spraying deposition, such as stream power and gas flow rate, which are more useful in process design. The most favorable results were obtained in [9] when the authors used regression analysis (RA) and response surface methodology (RSM) to evaluate the significance of four parameters: the Ar and $H_2$ flow rates; the current and powder feed rates in the atmospheric plasma spray process; but the power of the plasma stream also depends on the voltage, and ordinary air for plasma generation could have a different impact. Based on the foregoing reasoning, the goal of this work is to develop a mathematical model for the theoretical prediction of particle velocity in plasma spraying using ordinary air as the plasma-generating gas, including key factors such as current, plasma torch voltage, and air flow rate. In contrast to prior papers on the subject, the particle material used to deposit the anti-friction layer is Ni85Al15 powder. The ANOVA approach aids in determining the importance of each parameter in the regression equation. The proposed model of particle velocity prediction dealing with velocity optimization in future investigations demonstrated a disparity of less than 5%.

## 2. METHODOLOGY OF INVESTIGATION

Atmospheric plasma spraying was utilized in our experiment (SG-100 TAFA-Praxair, USA). Ordinary air serves as the main gas, while nitrogen serves as the carrier gas. [10] described the chemical composition and process of producing Ni85Al15 powders. The particle size of the powders is determined using the Cilas-1090 [11] instrument. Table 1 shows the fractional distribution of powders.

Table 1. The fraction distribution of particle Ni85Al15

| Code | Mean diameter (μm) | Particle size fraction, % | | | | | | | |
|---|---|---|---|---|---|---|---|---|---|
| | | 0 - 1 | 1 - 1.5 | 1.5 - 2.0 | 12 - 16 | 32 - 48 | 48 - 64 | 64 - 96 | 96 - 128 |
| Ni85Al15 | 64 | 7.5 | 8.9 | 4.1 | - | - | 72 | 4.2 | 3.2 |

Scanning electron microscopy combined with energy dispersive spectroscopy (SEM/EDS, SM-6510LV, Japan) was used to examine the surface morphology of the coatings and the topography of metallic particles. SEM investigation revealed that the feedstock particles had an uneven shape (Fig. 1). The Shimadzu HPV-1 high-speed camera is used to monitor the velocity of spraying particles [12]. The plasma spraying system is presented in Fig. 2. The plasma-generation gas is ordinary air. The carrier gas is also ordinary air. Ordinary air is a molecular gas that must be dissociated before it can be ionized. This means that ordinary air has greater enthalpy and thermal conductivity than argon plasma. Consequently, the molecular gases consume much higher input energy to become partially ionized. In this case, the powder Ni85AL15 is a good material recommendation for high-temperature coatings. This superalloy had a high oxidation resistance in the temperature range of up to 1250°C in the atmosphere.

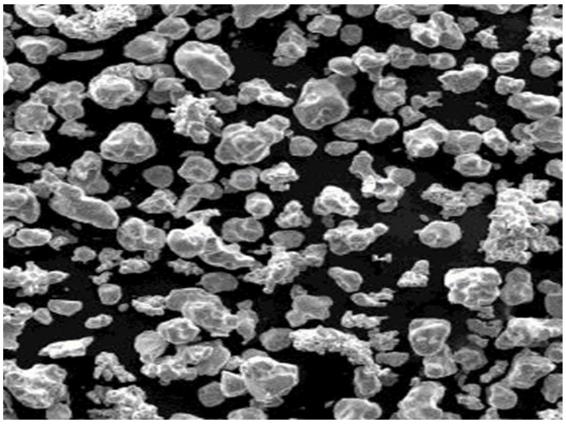

Fig. 1. The Irregular shape of particle

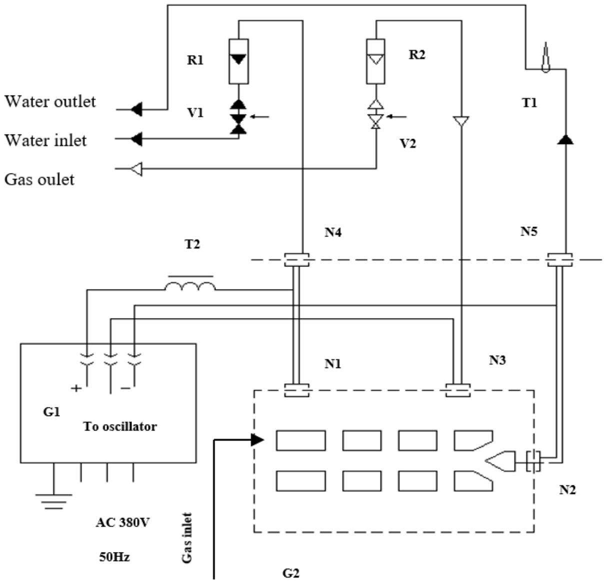

Fig. 2. The plasma spray system

The following is a brief summary of how the system works: G1 is the power source; G2 is the plasma torch; R1 and R2 are rotameters; V1 and V2 are valves; N1, N2, N3, N4, and N5 are nipples; T1 is the thermometer; and T2 is the throttle. The power source is a direct current source with a steep volt-ampere slope, an idle voltage of 300V, and a voltage adjustment range of 50 - 600V. The plasma arc is created in a two-step process. Water is used as the coolant, with inlet and exit valves, as well as rotameter R1. A T1 thermometer is used to monitor temperature and give data for calculating plasma jet enthalpy. This rotameter has a precision of 2.5. The intake water flow pressure is 0.4 - 0.6MPa. The primary and secondary gases are fed into the system via the valve V2. The rotameter R2 determines the gas flow rate. T2 is used to smooth out the current pulsation.

## 3. EXPERIMENT AND RESULT

### 3.1. Regression equation and the analysis of the variation

Table 2 shows the results of a series of experiments with different input spraying settings and particle velocity measurements.

Table 2. Result of Plasma Spraying of Powder PN 85Ni15Al

| No | Plasma current, I [A] | Potential, U [V] | Flow rate of air, G [g/s] | Particle velocity, V [m/s] |
|---|---|---|---|---|
| 1 | 130 | 140 | 0.55 | 18 |
| 2 | 130 | 160 | 0.75 | 40 |
| 3 | 130 | 195 | 0.34 | 62 |
| 4 | 130 | 200 | 1.13 | 73 |
| 5 | 130 | 210 | 1.42 | 84 |
| 6 | 130 | 220 | 1.76 | 97 |
| 7 | 130 | 225 | 1.95 | 105 |
| 8 | 130 | 240 | 2.72 | 140 |
| 9 | 130 | 250 | 2.92 | 152 |
| 10 | 150 | 150 | 0.55 | 36 |
| 11 | 150 | 185 | 0.84 | 67 |
| 12 | 150 | 205 | 1.13 | 78 |
| 13 | 150 | 207 | 1.42 | 85 |
| 14 | 150 | 220 | 1.76 | 99 |
| 15 | 150 | 240 | 2.41 | 128 |
| 16 | 150 | 245 | 2.92 | 153 |
| 17 | 150 | 250 | 3.17 | 167 |
| 18 | 180 | 145 | 0.55 | 33 |
| 19 | 180 | 160 | 0.75 | 49 |
| 20 | 180 | 180 | 0.84 | 65 |
| 21 | 180 | 202 | 1.13 | 82 |
| 22 | 180 | 220 | 1.76 | 104 |
| 23 | 180 | 240 | 2.60 | 140 |
| 24 | 180 | 250 | 3.17 | 170 |
| 25 | 220 | 150 | 0.55 | 43 |
| 26 | 220 | 160 | 0.75 | 53 |
| 27 | 220 | 190 | 0.94 | 76 |
| 28 | 220 | 200 | 1.13 | 84 |
| 29 | 220 | 220 | 1.76 | 106 |
| 30 | 220 | 245 | 2.60 | 143 |
| 31 | 220 | 260 | 3.17 | 172 |

The experimental results have been processing (Table 3) using Minitab software and were preliminarily analyzed. Because there are optimization requirements, we will use the 2nd tier planning form. We conduct a rough analysis with the quadratic regression equation full of coefficients.

Table 3. First Analysis of Experimental Results

| Term | Coef | SE Coef | T-Value | P-Value |
|---|---|---|---|---|
| Constant | 92.87 | 1.01 | 91.55 | 0.000 |
| I | 4.785 | 0.328 | 14.61 | 0.000 |
| U | 39.02 | 3.43 | 11.38 | 0.000 |
| G | 32.46 | 3.40 | 9.55 | 0.000 |
| $I^2$ | -1.547 | 0.383 | -4.04 | 0.001 |
| $U^2$ | -30.33 | 4.19 | -7.24 | 0.000 |
| $G^2$ | 9.56 | 3.02 | 3.17 | 0.005 |
| IU | -1.09 | 1.09 | -1.00 | 0.329 |
| IG | -0.75 | 1.12 | -0.67 | 0.508 |
| UG | 27.81 | 7.81 | 3.56 | 0.002 |

It was discovered that several coefficients with p-values larger than the precision of a = 0.05, especially two-way interactions between I and U and I and G, were removed, and the experimental findings were reanalyzed (Table 3). Notice that the coefficients of the double interaction between I and U, I and G with p-Value I*U = 0.329 and p-Value I*G = 0.508 respectively have values greater than the significance level by 5%, meaning that these coefficients are not necessary in the final regression equation. Remove these coefficients and recalculate the regression equation.

Table 4. Second Analysis of Experimental Results

| Term | Coef | SE Coef | T-Value | P-Value | VIF |
|---|---|---|---|---|---|
| Constant | 94.51 | 1.20 | 78.75 | 0.000 | |
| I | 4.856 | 0.317 | 15.31 | 0.000 | 1.27 |
| U | 35.01 | 4.32 | 8.10 | 0.000 | 144.33 |
| G | 36.59 | 4.27 | 8.57 | 0.000 | 168.78 |
| $I^2$ | -1.334 | 0.521 | -2.56 | 0.017 | 1.10 |
| $U^2$ | -33.03 | 5.70 | -5.79 | 0.000 | 73.59 |
| $G^2$ | 10.65 | 4.15 | 2.57 | 0.017 | 40.48 |
| UG | 26.6 | 10.8 | 2.47 | 0.021 | 285.38 |

The coefficient in column Coef is the coefficient of the regression equation in coded form, called X1, X2, X3 are 3 encoding variables for factors I, U, G, respectively, then the regression equation in coded form is:

$$\begin{aligned} V = 94.51 + 4.856X_1 + 35.01X_2 + 36.59X_3 \\ -1.334X_1^2 - 33.03X_2^2 + 10.65X_3^2 + 26.6X_2X_3 \end{aligned} \tag{1}$$

This time seeing that the coefficients of the whole regression equation make sense, conduct a variance analysis, calculate the regression equation. Analysis of the variance using the ANOVA method presented in Table 4. Subsequently, the regression equation in uncoded units introduced in (2).

Table 5. Analysis of Variance (ANOVA) from Experiment

| Source | DF | Adj SS | Adj MS | F-Value | P-Value |
|---|---|---|---|---|---|
| Model | 7 | 58310.8 | 8330.1 | 6000.79 | 0.000 |
| Linear | 3 | 55023.1 | 18341.0 | 13212.39 | 0.000 |
| I | 1 | 325.6 | 325.6 | 234.52 | 0.000 |
| U | 1 | 91.2 | 91.2 | 65.69 | 0.000 |
| G | 1 | 101.9 | 101.9 | 73.41 | 0.000 |
| Square | 3 | 394.0 | 131.3 | 94.61 | 0.000 |
| $I^2$ | 1 | 9.1 | 9.1 | 6.57 | 0.017 |

| | | | | | |
|---|---|---|---|---|---|
| $U^2$ | 1 | 46.6 | 46.6 | 33.58 | 0.000 |
| $G^2$ | 1 | 9.1 | 9.1 | 6.59 | 0.017 |
| 2-Way Interaction | 1 | 8.5 | 8.5 | 6.12 | 0.021 |
| UG | 1 | 8.5 | 8.5 | 6.12 | 0.021 |
| Error | 23 | 31.9 | 1.4 | | |
| Total | 30 | 58342.8 | | | |

Regression Equation in Uncoded Units:

$$\begin{aligned}&-347.2+0.3385I+3.703U-55.5G-0.000659I^2\\&-0.00918U^2+5.32G^2+0.314UG\end{aligned} \quad (2)$$

The degree of influence of these factors is shown by the graph below:

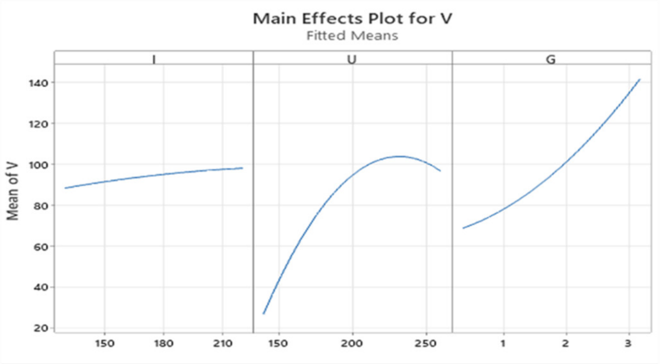

Fig. 3. Main Effects Plot for V

The analysis of the coefficients for the evaluation of the consistency of the regression equation (2) presented in Table 6.

Table 6. Analysis of the consistency

| S | $R^2$ | $R^2$ (adj) | $R^2$ (pred) |
|---|---|---|---|
| 1.17821 | 99.95% | 99.93% | 99.82% |

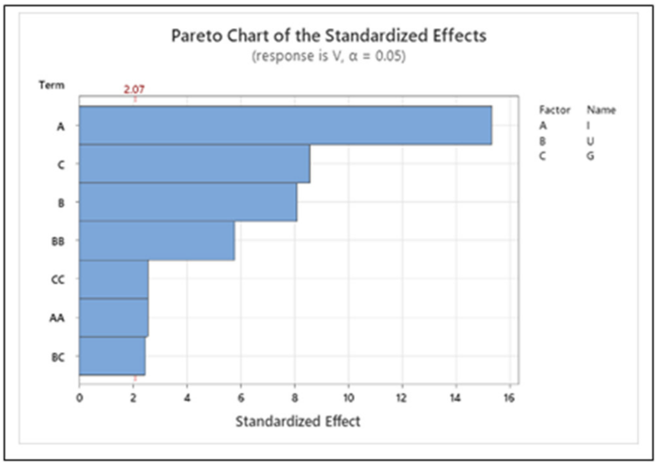

Fig. 4. Pareto chart [13] for input parameters

The suitability of the data was evaluated using a set of $R^2$, adjusted $R^2$, and predicted $R^2$ parameters. These values are all greater than 90%, indicating that the regression equation is perfectly compatible with the experimental data. The Pareto chart (Fig. 4) reveals that the plasma current (I), plasma voltage (U), and air flow rate (G) including $G^2$ and UG, are the factors that have the greatest influence on velocity (V).The other factors, such as $I^2$ and $U^2$ can be ignored.

This trend was also demonstrated by the normal plot (Fig. 5). As a result, the technical parameters I, U, and G are in the red. The large difference with the red line indicates that these factors have a considerable effect on the regression equation.

Fig. 5. Standard distribution chart of the standardized effect parameters

### 3.2. Preliminary optimization of the particle velocity

It is useful to analyze the conditions for the localization of the optimum area for particle velocity because it provides good coating quality, such as density, adhesion, cohesion strength, and so on [14]. Based on the experiment data, the following boundary conditions have been selected according to (3):

$$\begin{cases}130 \le I \le 220\\140 \le U \le 260\\0.34 \le G \le 3.17\end{cases} \quad (3)$$

The result of the preliminary optimization using the software Minitab, shown in Table 7 and Fig. 6.

Table 7. Optimization solution

| Solution | I | U | G | V Fit |
|---|---|---|---|---|
| 1 | 220 | 256.364 | 3.17 | 174.014 |

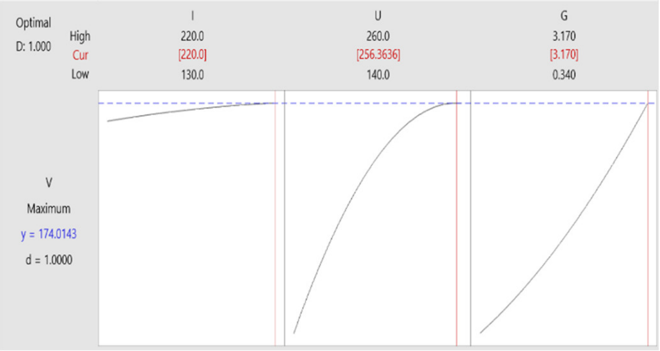

Fig. 6. Result of preliminary optimization of velocity

In Fig. 6, it is expected that the current of plasma and the flow rate of the gas have a monotonous influence on the particle velocity, while the voltage of plasma specifies the extreme. It is useful to conduct the complete experiment in the future to make reliable findings dealing with this assumption.

The first preliminary localization of the optimum in the planning area:

$$\begin{cases} I = 220 \\ U = 256.36 \\ G = 3.17 \end{cases}$$

## 4. ANALYSIS AND DISCUSSION

The voltage has the greatest impact on particle velocity, as shown by regression equation (2). The plasma current makes up the second level of effect. The air flow rate also had a favorable impact on particle velocity. An increase in the electric current in plasma causes a rise in the number of electrons, which raises the amount of ionization and generates more heat. The expansion of gas is made easier, and the velocity of the plasma jet, which includes the particles, is supported by the greater temperature. The particle will experience significant drag forces due to the high plasma jet velocity, which will cause it to accelerate. However, it is important to keep in mind that the particle velocity is lower than the plasma jet velocity. For example, while plasma spraying alumina powder, the particle in-flight velocity rose by 70m/s while the plasma jet velocity increased by 95m/s [15]. The mechanical compression, energy density, and thermal conductivity of the plasma jet all increase as the gas flow rate rises, encouraging the plasma jet's velocity to accelerate more quickly. According to the dynamic phenomenon, an increase in gas flow rate contributes to a rise in the plasma stream's overall momentum, which raises particle velocity. Since the mathematical model does not include a lot of variables, notably the size distribution, the issue of the size and density of the particle material as well as the fractional size distribution is still up for debate. However, in reality, no powder manufacturer offers a detailed specification on the size distribution. Size distribution and manufacturing costs are inextricably linked. In the future, it will be beneficial to conduct a number of experiments involving the plasma spraying of various powder materials to gather information on their mechanical and physical properties in order to enhance the approach for predicting the particle velocity in terms of optimization. For the sake of simplicity, all mathematical models assume that particles have a spherical shape. But in the production of the spraying particles, they can have different morphologies. This issue also contributes to some errors in the theoretical calculation of the velocity. To cover the gap between the theoretical prediction and the experiment, the empirical formula can be used as the predominant solution in the context.

## 5. CONCLUSIONS

In the case of deposition powder Ni85Al15, the influence of some key parameters, such as plasma jet power, gas flow rate, and particle average size, on particle velocity is observed in atmospheric plasma spraying using ordinary air as the plasma generation gas. The increase in plasma power and the flow rate of gas help increase the in-flight velocity of the particles. The necessary condition for the deposition is the so-called critical velocity, and this value will decide the efficiency of the processes. The mathematical model using the method of multi-criteria planning and design of experiments is well adapted to the experiment data and can be recommended to find the optimum of the particle velocity when some other related parameters will be involved, and a more complete planning experiment can be designed in a future study. It is useful to make some corrections to the theoretical calculations of the particle velocity, taking into account the morphology of the particles and their size distribution.

## CONFLICTS OF INTEREST

Authors identify and declare that they do not have any conflict of interest.

## REFERENCES

[1]. B. Guduri., M. Cybulsky., G. R Pikrell, R.C. Batra, "Adaptive process control for achieving consistent particle's state in atmospheric plasma spray process," *SN Applied Science, Springer Nature Journal,* 3, 294, 2021. https://10.1007/s42452-021-04296-y.

[2]. Rong Gen Neo, Kaiqiang Wu, Sung Chyn Tan, Wei Zhou, "Effect of Spray Distance and Powder Feed Rate on Particle Velocity in Cold Spray Processes," *Metals,* 12, 75, 2022. https://doi.org/10.3390/met12010075.

[3]. Francois Raletz, Michel Vardelle, Guillaume Ezo'o, "Critical particle velocity under cold spray conditions," *Surface & Coating Technology*, 201(5), 1942-1947, 2006. doi: 10.1016/j.surfcoat.2006.04.061.

[4]. Jingwei Wu, Hongyuan Fang, Sanghoon Yoon, Changhee Lee, Hyung Jun Kim, "Critical Velocities for High- Speed Particle Deposition in Kinetic Spraying," *Materials Transactions*, 47(7), 1723-1727, 2006. doi: 10.2320/matertrans.47.1723.

[5]. Y. V Kurochkin, Y. N Demin, S. I Soldatenknov, "Demonstration of the Method of Cold Gasdynamic Spraying of Coatings," *Chemical and Petroleum Engineering*, 38(3-4), 245-248, 2002. https://link.springer.com/journal/10556/volumes-and-issues/38-3.

[6]. Pei Wei, Zhengying Wei, Guanxi Zhao, Y Bai, Chao Tan, "Effect of Processing Parameters on Plasma Jet and In-Flight Particles Characters in Supersonic Plasma Spraying," *High Temperature Materials and Processes*, 35(8), 775-786, 2016. doi: 10.1515/htmp-2015-0077.

[7]. L. Alonso, M.A. Garrido-Maneiro, P. Poza, "A study of the parameters affecting the particle velocity in cold-spray: Theoretical results and comparison with experimental data," *Additive Manufacturing*, 67, 103479, 2023. https://doi.org/10.1016/j.addma.2023.103479.

[8]. K. Bobzin, M. Oter, M. A. Knoch, I. Alkashli, U. Reisgen, O. Mokrov, O. Lysnyi, "Simulation of the Particle Melting Degree in Air Plasma Spraying," in *14th High-Tech Plasma Processes Conference, IOP Conf.Series: Journal of Physics: Conf Series,* 825, 012002, 2017.

[9]. R. C. Batra, Unchalisa Taetragool, "Numerical techniques to find optimal input parameters for achieving mean particles' temperature and axial velocity in

atmospheric plasma spray process," *Scientific Reports, Nature Research*, 10(1): 21483, 2020. https://doi.org/10.1038/s41598-020-78424-w.

[10]. D. Kotoban, S. Grigoriev, I. Shishkovsky, "Study of 3D laser cladding for Ni85Al15 superalloy," in *8th International Conference on Photonic Technologies LANE 2014, Physics Procedia*, 56, 262-268, 2014. doi:10.1016/j.phpro.2014.08.170.

[11]. Duong Vu, Quy Le Thu, "The Correlation Between Main Parameters in the Air-Plasma Spraying of Fe-based Amorphous Coatings," in *The Proceedings of the International Conference on Advanced Mechanical Engineering, Automation and Sustainable Development (AMAS 2021)*, November 04-07,2021, Ha Long city, Vietnam, Lecture Notes in Mechanical Engineering, Springer Publisher, 499-506,2022. doi: 10.1007/978-3-030-99666-6_72.

[12]. N. A Buchman, C. Cierpka, C. J Kahler, "Ultra high speed 3D astigmatic particle tracking velocimetry: application to particle-laden supersonic impinging jets," *Exp fluids*, 55:1842, 2014. doi 10.1007/s00348-014-1842-1.

[13]. Mohammad Tabatabaei, Alberto Lovison, Matthias Tan, Markus Hartikainen, Kaisa Miettinen, "ANOVA-MOP : ANOVA Decomposition for Multiobjective Optimization," *SIAM Journal on Optimization*, 28(4), 2018. https://doi.org/10.1137/16M1096505.

[14]. Rong Gen Neo, Kaiqiang Wu, Sung Chin Tan,Wei Zhou, "Effect of Spray Distance and Powder Feed Rate on Particle Velocity in Cold Spray Processes," *Metals,* 12(1), 75, 2022. https://doi.org/10.3390/met12010075.

[15]. Airingas Suopys, Viktorija Grigaitiene, Liutauras Marcinauskas, Romualdas Kezelis, Rolandas Uscila, Mindaugas Aikas, "Influence of Plasma Torch Power on the Plasma Jet Properties and Microstructure of Alumina Coatings," *Coatings*, 12, 934, 2022. https://doi.org/10.3390/coatings12070934.